Science and Engineering Research Council
Rutherford Appleton Laboratory
Chilton DIDCOT Oxon OX11 0QX

RAL-93-074

Probing Lepton Number Violation Via Majorana Neutrinos at Hadron Supercolliders

A Datta M Guchait and A Pilaftsis

November 1993

RAL/93-074

October 1993

PROBING LEPTON NUMBER VIOLATION VIA MAJORANA NEUTRINOS AT HADRON SUPERCOLLIDERS

A. Datta[a], M. Guchait[a] and A. Pilaftsis[b]

[a] Physics Department, Jadavpur University, Calcutta 700 032, India

[b] Rutherford Appleton Laboratory, Chilton, Didcot, Oxon, OX11 0QX, UK.

ABSTRACT

The possibility of discovering heavy Majorana neutrinos and lepton number violation via the like sign dilepton signal at hadron supercolliders is investigated. The cross-sections for the production of these neutrinos singly as well as in pairs are computed both in three and four generation scenarios within the framework of the gauge group $SU(2)_L \otimes U(1)_Y$ and the dominant processes are identified. The suppression of the Standard model background by suitable kinematical cuts is also discussed.

I. Introduction

The present limits on the neutrino masses [1] reveal that even if these masses are nonvanishing, they must be unnaturally small compared to the corresponding quark or charged lepton masses. An attractive solution to this naturalness problem was inspired by the "see-saw" mechanism [2] with the assumption that the neutrinos are Majorana fermions. In a simple "see-saw" model with one generation of quarks and leptons, one obtains two massive Majorana neutrinos, ν and N, having masses $m_\nu \simeq m_D^2/m_M$ and $m_N \simeq m_M$. Thus if the Dirac mass of neutrinos m_D is of the order of a typical quark or lepton mass and the Majorana mass $m_M \gg m_D$, then m_ν can indeed be very small.

Originally the "see-saw" mechanism was contemplated in the context of models (e.g. grand unified theories (GUT's) or left-right symmetric models [3]) where the scale m_M is several orders of magnitude larger than the electroweak scale. In such models the heavy neutrino mass is much beyond the reach of the planned hadron supercolliders. Recently, however, simple extensions of the Glashow-Salam-Weinberg standard model (SM) with Majorana mass terms for the neutrinos have received much attention [4–6,10,11]. These models based on the gauge group $SU(2)_L \otimes U(1)_Y$ and $m_M \sim 1$ TeV, predict heavy neutrinos well within the striking ranges of SSC* and LHC. In particular, the observation of the spectacular lepton-number violating decays of the heavy neutrinos via the like sign dilepton (LSD) channel is of great experimental interest.

The coupling of the heavy neutrinos with W, Z and Higgs (H) bosons are, however, also naturally small. In an one generation "see-saw" model the suppression factor $\xi = m_D/m_M$ turns out to be too small even for $m_M \sim 1$ TeV, suppressing thereby the

*After completing our work, we became aware of the disappointing news about the cancellation of the SSC project. However, our forthcoming analysis of the isolation of lepton-number violating signals from the SM background will show to be more relevant for the LHC collider.

production cross-sections of these neutrinos. It has, however, been pointed out that in realistic three generation models, the neutrino masses are described by a 6×6 matrix and the simple suppression as mentioned above may not work [6,10,7]. But there are stringent experimental bounds on these suppression factors from LEP data as well as from low energy experiments [8,9] which forces us to accept that this factor cannot be very large.

The purpose of the present work is to study the feasibility of observing the LSD signals at LHC and SSC by taking the most recent bounds on the mixing angles into account. In Section II we estimate the cross sections for the production of heavy Majorana neutrinos singly as well as in pairs, via all possible channels. We then compute the cross section for the LSD signal (using a parton level Monte Carlo calculation) for the dominant process, which turns out to be $pp \rightarrow W^* \rightarrow lNX$, followed by the lepton number violating decay of the heavy neutrino N. The kinematical cuts required to suppress the SM backgrounds arising primarily due to heavy flavour production followed by cascade decays are also discussed.

The neutrino counting at LEP strongly suggests that there are only three light neutrinos within the framework of the SM. In an attempt to demonstrate that the existence of a fourth family still remains a viable possibility, it was shown that one can construct a simple extension of the SM with two naturally heavy Majorana neutrinos belonging to the fourth generation [5]. It was subsequently pointed out that the coupling of these new neutrinos with W, Z and H are also naturally large [6]. As a result these neutrinos can be copiously produced at hadron colliders. Production cross sections for heavy Majorana neutrino pairs were calculated and they were found to be rather large [6]. The number of LSD's was also estimated qualitatively.

In Section III we shall take up the question of producing the LSD signal in the context of the above four generation model in further details. The SM backgrounds and the relevant kinematical cuts required to suppress it is also discussed. Our conclusions

will be summarized in section IV.

II. *LSD*'s in a three generation model

II.1 The model

Adopting the notation of Ref. [10], the relevant interaction Lagrangian involving charged current is given by (summation convention implied)

$$\mathcal{L}_{int}^{W-\nu_M-l} = -\frac{g_W}{\sqrt{2}} W^{-\mu}\Big[\bar{l}_i\gamma_\mu \mathrm{P}_L(B_{l_ij}\nu_j + B_{l_i\alpha}N_\alpha)\Big] + H.c.\,, \tag{1}$$

where $\mathrm{P}_L = (1-\gamma_5)/2$, g_W is the coupling constant of $SU(2)_L$ and l, ν, N and W are respectively the lepton, light neutrino, heavy neutrino and the W-boson field. The latin indices i, j, etc.$= 1,\ldots,n_G$, where n_G denotes the number of generations, are used for charged leptons and light neutrinos, while the greek indices α, β, etc.$= n_G+1,\ldots,2n_G$ indicate heavy Majorana neutrinos. The neutral current interaction is given by

$$\begin{aligned}\mathcal{L}_{int}^{Z-\nu_M-\nu_M} &= -\frac{g_W}{4\cos\theta_W} Z^\mu\Big[\bar{\nu}_i\gamma_\mu(i\mathrm{Im}C_{ij} - \gamma_5\mathrm{Re}C_{ij})\nu_j \\ &+ \Big\{\bar{\nu}_i\gamma_\mu(i\mathrm{Im}C_{i\alpha} - \gamma_5\mathrm{Re}C_{i\alpha})N_\alpha + H.c.\Big\} \\ &+ \bar{N}_\alpha\gamma_\mu(i\mathrm{Im}C_{\alpha\beta} - \gamma_5\mathrm{Re}C_{\alpha\beta})N_\beta\Big].\end{aligned} \tag{2}$$

B and C in Eqs. (1) and (2) are $n_G\times 2n_G$ and $2n_G\times 2n_G$ dimensional matrices, respectively, which obey a number of useful identities. More details can be found in [10,11]. For our purpose it is sufficient to remember that the coupling matrix $B_{i\alpha}$ is $\mathcal{O}(\xi)$ while the matrix $C_{\alpha\beta}$ is $\mathcal{O}(\xi^2)$. It is, therefore, clear that the Z-mediated pair production of heavy neutrinos are more severely suppressed compared to the W-mediated Nl production due to (i) phase-space suppression and (ii) a smaller mixing angle.

The interaction of the Majorana neutrinos with the Higgs boson is governed by the Lagrangian

$$\begin{aligned}\mathcal{L}_{int}^{H-\nu_M-\nu_M} &= -\frac{g_W}{4M_W}\, H\Big[\bar{\nu}_i\Big((m_i+m_j)\mathrm{Re}C_{ij} \;+\; i\gamma_5(m_j-m_i)\mathrm{Im}C_{ij}\Big)\nu_j \\ &+\; 2\,\bar{\nu}_i\Big((m_i+m_\alpha)\mathrm{Re}C_{i\alpha} \;+\; i\gamma_5(m_\alpha-m_i)\mathrm{Im}C_{i\alpha}\Big)N_\alpha \\ &+\; \bar{N}_\alpha\Big((m_\alpha+m_\beta)\mathrm{Re}C_{\alpha\beta} \;+\; i\gamma_5(m_\beta-m_\alpha)\mathrm{Im}C_{\alpha\beta}\Big)N_\beta\Big]. \qquad (3)\end{aligned}$$

where m_α (m_i) stands for the mass of the αth (ith) heavy (light) neutrino. It is clear from Eq. (3) that the coupling of the heavy neutrinos with the Higgs boson will be enhanced by a factor m_α/M_W. But a similar enhancement also works, up to a different γ_5 structure, for the couplings of these Majorana neutrinos to the longitudinal Z boson or the would-be Goldstone boson z in the Feynman-'t Hooft gauge [10]. Therefore, apart from the resonance enhancement that the production of a heavy on–shell Higgs boson and its subsequent decay into a pair of heavy neutrinos may introduce, a priori there is no obvious difference in the coupling strengths of the Higgs mediated and the Z-mediated processes.

The bounds on the mixing angles are given in Ref. [9] using both LEP results and low-energy constraints. For definiteness, we have have used the following upper bounds from the joint fits of [9]:

$$(s_L^{\nu_e})^2 \;<\; 0.01\;, \qquad (4)$$

$$(s_L^{\nu_\mu})^2 \;<\; 0.01\;, \qquad (5)$$

$$(s_L^{\nu_\tau})^2 \;<\; 0.065\;. \qquad (6)$$

It should be noted that these limits are obtained under the assumption that each lepton e, μ or τ couples to only one heavy neutrino with significant strength. However, in the notation of eq. 1 we can make the following identification [9]

$$(s_L^{\nu_l})^2 \;\equiv\; \sum_\alpha |B_{l\alpha}|^2\;. \qquad (7)$$

Since τ lepton identification may be rather complicated in hadron supercolliders, we restrict our analysis to LSD pairs of the types: e^+e^+, e^-e^-, $\mu^+\mu^+$, $\mu^-\mu^-$, $e^+\mu^+$ and $e^-\mu^-$ and will probe the prospects of observing lepton-number violation, after isolating the background. On the other hand, the LSD signal comprising of stable leptons which originates from equal-sign τ leptons will eventually be diluted by the small leptonic branching ratio of τ.

II.2 The cross sections

The lepton-number violating LSD signal may potentially arise due to the following processes (see Figs. 1-3):

$$\begin{aligned}
&\text{A.} \quad pp \rightarrow W^*W^* \rightarrow ll \,, \\
&\text{B.} \quad pp \rightarrow W^* \rightarrow lN_\alpha \,, \\
&\text{C.} \quad pp \rightarrow W^*Z^* \rightarrow lN_\alpha \,, \\
&\text{D.} \quad pp \rightarrow W^*\gamma^* \rightarrow lN_\alpha \,, \\
&\text{E.} \quad pp \rightarrow Z^* \rightarrow N_\alpha N_\beta \,, \\
&\text{F.} \quad pp \rightarrow W^*W^* \rightarrow N_\alpha N_\beta \,, \\
&\text{G.} \quad pp \rightarrow Z^*Z^* \rightarrow N_\alpha N_\beta \,, \\
&\text{H.} \quad pp \rightarrow \mathrm{gg} \rightarrow H^*,\ Z^* \rightarrow N_\alpha N_\beta \,.
\end{aligned}$$

The relevant differential cross sections $(d\hat{\sigma}_A/d\hat{t} - d\hat{\sigma}_H/d\hat{t})$ for the parton subscatterings are listed below

$$\frac{d\hat{\sigma}_A}{d\hat{t}} = \frac{\pi\alpha_W^2|B_{l\alpha}^2|^2}{4\hat{s}} \frac{m_\alpha^2\,(m_\alpha^2 - m_\beta^2)^2}{M_W^4} \left[\frac{\hat{t}}{(\hat{t}-m_\alpha^2)(\hat{t}-m_\beta^2)} + \frac{\hat{u}}{(\hat{u}-m_\alpha^2)(\hat{u}-m_\beta^2)}\right]^2, \quad (8)$$

$$\frac{d\hat{\sigma}_B}{d\hat{t}} = \frac{\pi\alpha_W^2|B_{l\alpha}|^2}{12\hat{s}^2} \frac{\hat{t}(\hat{t}-m_N^2)}{(\hat{s}-M_W^2)^2}\,, \quad (9)$$

$$\frac{d\hat{\sigma}_C}{d\hat{t}} = \frac{\pi\alpha_W^2|B_{l\beta}C_{\beta\alpha}|^2}{2\hat{s}^2}\,\frac{m_N^4}{M_W^4}\left[\frac{\hat{s}-m_N^2}{m_N^2-\hat{t}} + \frac{\hat{t}(\hat{t}-3m_N^2)}{(\hat{t}-m_N^2)^2}\right]$$
$$= \mathcal{O}(\xi^6)\,, \tag{10}$$

$$\frac{d\hat{\sigma}_D}{d\hat{t}} = \frac{\pi\alpha_W\alpha_{em}|B_{l\alpha}|^2}{2\hat{s}^2}\,\frac{m_N^2}{M_W^2}\left(-1 + \frac{m_N^2}{\hat{s}} - \frac{\hat{s}-m_N^2}{\hat{t}}\right), \tag{11}$$

$$\frac{d\hat{\sigma}_E}{d\hat{t}} = \frac{\pi\alpha_W^2|C_{\alpha\beta}|^2}{24c_W^4\hat{s}^2}\,\frac{(g_V^q)^2+(g_A^q)^2}{(\hat{s}-M_Z^2)^2}\left[(\hat{s}+\hat{t}-m_N^2)^2 + (\hat{t}-m_N^2)^2 - 2m_N^2\hat{s}\right], \tag{12}$$

$$\frac{d\hat{\sigma}_F}{d\hat{t}} = \frac{\pi\alpha_W^2|C_{\alpha\beta}|^2}{2\hat{s}^2}\,\frac{m_N^4}{M_W^4}\left[\frac{M_H^2}{m_N^2}\,\frac{M_H^2(\hat{s}-4m_N^2)}{(\hat{s}-M_H^2)^2+M_H^2\Gamma_H^2} + \frac{\hat{s}(\hat{s}-2m_N^2)-4m_N^4}{2\hat{u}\hat{t}}\right.$$
$$- 1 - \frac{1}{2}\left(\frac{m_N^4}{\hat{t}^2} + \frac{m_N^4}{\hat{u}^2}\right)$$
$$\left. + \frac{2M_H^2(\hat{s}-M_H^2)}{(\hat{s}-M_H^2)^2+M_H^2\Gamma_H^2}\left(\frac{m_N^2(\hat{s}-2m_N^2)}{\hat{u}\hat{t}} - 2\right)\right], \tag{13}$$

$$\frac{d\hat{\sigma}_G}{d\hat{t}} = \frac{\pi\alpha_W^2|C_{\alpha\beta}|^2}{2\hat{s}^2}\,\frac{m_N^4}{M_W^4}\left[\frac{M_H^2}{m_N^2}\,\frac{M_H^2(\hat{s}-4m_N^2)}{(\hat{s}-M_H^2)^2+M_H^2\Gamma_H^2} + \frac{(\hat{s}-4m_N^2)^2}{4\hat{u}\hat{t}}\right.$$
$$\left. - \left(\frac{m_N^2(\hat{s}-2m_N^2)}{2\hat{u}\hat{t}} - 1\right)^2\right], \tag{14}$$

$$\frac{d\hat{\sigma}_H}{d\hat{t}} = \frac{\alpha_S^2\alpha_W^2|C_{\alpha\beta}|^2}{1152\pi\hat{s}}\,\frac{m_N^2}{M_W^4}\left(|F^H(\frac{m_t^2}{\hat{s}})|^2\,\frac{\hat{s}(\hat{s}-4m_N^2)}{(\hat{s}-M_H^2)^2+M_H^2\Gamma_H^2} + \frac{9}{4}\,|F^Z(\frac{m_t^2}{\hat{s}})|^2\right), \tag{15}$$

with

$$F^H(x) = 3x\left[\,2 + (4x-1)K^H(x)\,\right],$$
$$K^H(x) = \theta(1-4x)\frac{1}{2}\left[\ln\left(\frac{1+\sqrt{1-4x}}{1-\sqrt{1-4x}}\right) + i\pi\right]^2 - \theta(4x-1)2\left[\sin^{-1}\left(\frac{1}{2\sqrt{x}}\right)\right]^2,$$

and

$$F^Z(x) = -(-1)^{T_z^q+1/2}\,K^Z(x),$$
$$K^Z(x) = \theta(1-4x)4x\left\{\left[\cosh^{-1}\left(\frac{1}{2\sqrt{x}}\right)\right]^2 - \frac{\pi^2}{4} + i\pi\cosh^{-1}\left(\frac{1}{2\sqrt{x}}\right)\right\}$$
$$- \theta(4x-1)4x\left[\sin^{-1}\left(\frac{1}{2\sqrt{x}}\right)\right]^2.$$

In Eqs. (8)–(15), $\hat{s}$, $\hat{t}$, $\hat{u}$ are the relevant Mandelstam variables defined at the subprocess level, Γ_H is the total width of the Higgs boson, and $g_V^q = -T_z^q + 2Q_q s_W^2$, $g_A^q = -T_z^q$, where

the third component of the weak isospin T_z^q of the $u(d)$-type quarks and the corresponding electric charge of them Q_q (in units of $|e_{em}|$) are respectively given by $T_z^{u(d)} = +(-)1/2$ and $Q_{u(d)} = 2/3(-1/3)$. Furthermore, Eqs. (8), (10),(11), (13), (14) have been computed using the equivalence theorem. This simplification occurs at high energies (i.e. $\sqrt{\hat{s}} \gg M_W$) where one is allowed to substitute the vector bosons W_L and Z_L by the corresponding would-be Goldstone bosons w and z in the Landau gauge and take the limit $g_W \to 0$ by keeping $g_W/2M_W = 1/v$ fixed. This approach shown in Figs. 1–3 gives reliable results for heavy fermions with masses $m_N \gg M_W$ [12]. In the context of three generation models, one can further simplify the calculations by assuming that the mass difference of each pair of heavy neutrinos, e.g. N_α and N_β, is very small compared to the masses m_α and m_β, i.e. $m_\alpha,\ m_\beta \sim m_N$. The above approximation has explicitly been employed in Eqs. (9)–(15).

We have calculated the cross sections for the positively charged LSD pairs arising from the pp process by using the parton distribution functions of Ref. [13], $m_t = 150$ GeV and $M_H = 200 - 1000$ GeV. The heavy neutrino masses are kept as free phenomenological parameters. Then, the total cross sections for the processes (B)–(C) given above are evaluated by using the generic formula

$$\sigma_{tot}(l^+l^+) \;=\; \frac{1}{9}\, R^{(1)} \sum_{ab} \int dx_1 dx_2\; f_a^p(x_1) f_b^p(x_2) \int d\hat{t}\; \frac{d\hat{\sigma}^0}{d\hat{t}}\; \frac{\int d\Gamma(N_\alpha \to l^+ q\bar{q}')}{\Gamma(N_\alpha \to l q\bar{q}')}, \qquad (16)$$

where $\hat{\sigma}^0 = \hat{\sigma}/|B_{l\alpha}|^2$ and

$$R^{(1)} \;=\; \sum_{l_i l_j = e,\mu} \sum_{\alpha} \frac{|B_{l_i\alpha}|^2 |B_{l_j\alpha}|^2}{\sum\limits_{l_m} |B_{l_m\alpha}|^2}. \qquad (17)$$

In models with three families, one can use the identity that $C_{\alpha\alpha} = \sum_l |B_{l\alpha}|^2$ and the fact that $|B_{\tau\alpha}|^2/C_{\alpha\alpha} \leq 1$ to obtain a reasonable upper bound of

$$R_{3G}^{(1)} \;\leq\; (s_L^{\nu_e})^2 \;+\; (s_L^{\nu_\mu})^2\,, \qquad (18)$$

where the subscript $3G$ denotes three generations.

For the processes (E)–(H) one uses the more involved convoluting integral similar to Eq. (16)

$$\sigma_{tot} = \frac{4}{81} R^{(2)} \sum_{ab} \int dx_1 dx_2 \, f_a^p(x_1) f_b^p(x_2) \int d\hat{t} \frac{d\hat{\sigma}^0}{d\hat{t}} \frac{\int d\Gamma(N_\alpha \to l_i q_1 \bar{q}_1')}{\Gamma(N_\alpha \to l_i q_1 \bar{q}_2')} \times \frac{\int d\Gamma(N_\beta \to l_j q_2 \bar{q}_2')}{\Gamma(N_\beta \to l_j q_2 \bar{q}_2')}, \tag{19}$$

where $\hat{\sigma}^0 = \hat{\sigma}/|C_{\alpha\beta}|^2$ and

$$R^{(2)} = \sum_{l_i l_j = e,\mu} \sum_{\alpha\beta} \frac{|B_{l_i\alpha}|^2 |C_{\alpha\beta}|^2 |B_{l_j\beta}|^2}{\sum_{l_m l_k} |B_{l_m\alpha}|^2 |B_{l_k\beta}|^2}. \tag{20}$$

Eq. 19 is only valid if LSD's of both charges are considered. Using similar assumptions and Schwartz's inequality, i.e. $C_{\alpha\alpha} C_{\beta\beta} \geq |C_{\alpha\beta}|^2$, one arrives at the simple result

$$R_{3G}^{(2)} \leq \left((s_L^{\nu_e})^2 + (s_L^{\nu_\mu})^2 \right)^2 \tag{21}$$

The processes (A), (C), (D), (F) and (G) have been computed by using the effective vector boson approximation ($EVBA$) [14]. As we are interested in producing heavy neutrinos with masses $m_N \geq 200 - 300$ GeV, being equivalent with a threshold invariant mass of $\sqrt{\hat{s}_{thr}} \geq 400 - 500$ GeV (without including kinematical cuts relevant for the SM background), it has been demonstrated in [15] that $EVBA$ can safely be applied by only using the distribution functions of the longitudinal vector bosons. Furthermore, adapting the numerical results of [16], one can readily see that the subreaction $W_L\gamma \to lN_\alpha$ will dominate for large fermion masses ($m_N \geq 200$ GeV) by a factor of 10 at least against other subprocesses of the type, e.g., $W_L Z_T$, $W_T Z_L$, $W_T Z_T \to lN_\alpha$ etc.

Our results are summarized in Table I. In consistency with what has been discussed before, we find from this table that only processes (B) and (D) can have sizable cross sections, i.e. sufficiently large to yield observable LSD signals at LHC or SSC. The process (A) [17], though free from background sources, is, however, suppressed by an additional factor $R_{3G}^{(1)2} \simeq 10^{-4}$. In the next subsection we shall calculate the LSD cross sections and compare them with the SM background.

II.3 The *LSD* signal from $pp \to W^* \to lN_\alpha$ and the *SM* background

From Table I one easily concludes that the dominant contribution to the LSD signal comes from $pp \to W^* \to lN_\alpha$ and $pp \to W^*\gamma^* \to lN_\alpha$. However, the cross sections for the latter process is based on the $EVBA$. Being conservative we have not included this process in our analysis . The numerical estimate presented in Table I for this process indicates that this exclusion is not likely to alter our conclusions at the order of magnitude level.

As has already been discussed in Ref. [18], the dominant SM background arises from the $t\bar{t}$ production:

$$pp \;\to\; t\bar{t} \;\to\; (bl^+\nu_l)(\bar{b}q_iq_j)\;; \qquad \bar{b} \;\to\; l^+\nu_l c\;. \tag{22}$$

where q_iq_j are the quarks u, d, s or c in appropriate combinations. It is also important to notice that the background from $c\bar{c}$, $b\bar{b}$ pairs or from $B^0 - \bar{B}^0$ mixing will be more severely suppressed by the lepton isolation cut (see Ref. [18] for more details). We have, however, updated the analysis of Ref. [18] by using the parton density functions of Ref. [13].

The signal can, in principle, be distinguished from the background by the following criteria:

i) The characteristics of the dilepton pairs (p_T distribution, invariant mass etc.)

ii) The characteristics of the jets in the final state. For example, at the parton level the number of jets in the final state is two (four) for the signal (background). Any conclusion based on this without taking jet fragmentation etc. into account, however, may turn out to be misleading. Since all calculations in this work are based on a parton level Monte Carlo, we shall not use the specific features of the jets.

iii) The signal involves only visible energy while the background has missing p_T due to the presence of stable neutrinos in the final state. However, the missing p_T spectrum (see

Fig. 4), as expected, is not very hard due to the neutrinos arising from b decay. To what extent this missing p_T can be utilized in distinguishing the signal from the background, depends crucially on the accuracy in measuring the total p_T in the final state. There is no clear information on this point at the moment.

We have, therefore, based our analysis of improving the signal to background ratio by solely using the characteristics of the dilepton pairs. In any case, the simultaneous exploitation of all the three kinematical features listed above can only strengthen our conservative conclusions regarding the feasibility of observing the lepton number violation at hadron colliders.

As is well known the small mass of the bottom quark relative to the large p_T of the decay lepton ensures that the lepton emerges together with the decay hadrons within a narrow cone [19], while the leptons arising from the semileptonic decay of the heavy neutrino or the top quark are well isolated. Hence, the background coming from the decay sequence in Eq. (22) can be suppressed by a suitable lepton isolation criterion

$$E_{AC}^{T} \quad < \quad 10 \text{ GeV}, \tag{23}$$

applied to both leptons appearing in the final state. Here E_{AC}^{T} represents the total transverse energy accompanying the lepton track within a narrow cone of half angle 0.4 radian.

Fig. 5 shows the signal and the background cross sections against p_{T2}, the transverse momentum of the softer lepton. In addition to the above isolation cut, p_T cuts $p_{T2} >$ 20 GeV and $p_{T1} > 40$ GeV has been applied, where p_{T1} is the transverse momentum of the harder lepton.

It was pointed out in [20] that the isolation cut becomes more effective with increasing p_{T2}. This is reflected in Fig. (5) where the background cross section goes down drastically by increasing the p_{T2} cut. It was, however, observed in Ref. [18] that this dramatic reduction (obtained from a parton level Monte Carlo) may not be completely

realistic due to effects like jet fragmentation. A detailed study of the combined effect of the lepton p_T cut and the isolation cut on the background using the $ISAJET$ program [21] was carried out in Ref. [22]. The main result of Ref. [22] was that for the isolation cut of $E_{AC}^T < 10$ GeV, a kinematical cut $p_{T2} > 80$ GeV suffices to kill the background completely.

Since the background can be eliminated, the prospect of detecting lepton-number violation at hadron colliders is essentially governed by the size of the LSD signal. This signal crucially depends on the magnitude of the mixing-angle quantity $R_{3G}^{(1)}$ and m_N. Using the kinematical cuts $E_{AC}^T < 10$ GeV, $p_{T2} > 80$ GeV, the present conservative upper bound on $R_{3G}^{(1)} \simeq 0.02$ and an integrated luminosity 4×10^5 pb^{-1}/yr for LHC, we obtain the following results:

m_N [GeV]	No of LSD's
200	48
300	32
400	16

(24)

If LSD's of both signs are considered the numbers in the left column will be multiplied by a factor of 1.5 (approximately). We remind the reader that in reality signals larger than the above conservative estimates may be obtained if a) $|B_{l\alpha}|^2$ happens to be somewhat larger; as has already been mentioned, this possibility is not totally excluded by the data, if the possibility of accidental cancellations is taken into account [8,9] b) contributions from $pp \to W^*\gamma^* \to lN_\alpha$ are included (a detailed calculation without using $EVBA$ is, however, desirable) c) the kinematical cuts used in computing the cross sections can be somewhat relaxed by exploiting other characteristics (see (ii) and (iii) above) in separating the signal from the background. On the other hand, should $|B_{l\alpha}|^2$ (and $R_{3G}^{(1)}$) happen to be much smaller than the existing bound, the LSD signal may remain elusive at hadron colliders.

The situation at SSC, however, is inconclusive at the moment. The cross sections

happen to be larger typically by a factor 2 to 2.5 for parameters and kinematical cuts as given above. This enhancement is not adequate to compensate for the much smaller integrated luminosity (10^4 pb^{-1}/yr). Detailed analysis of all the avenues for enhancing the signal as listed above is, therefore, called for. In any case, this is also desirable in order to assess the feasibility of probing larger neutrino masses at the *LHC*.

III. A four-generation model with heavy Majorana neutrinos

III.1 The model

It was emphasized in [6] that the model in Ref. [5] predicts large couplings of heavy Majorana neutrinos belonging to the fourth generation with Z and H bosons. Hence, the production cross section of these neutrinos, here-after denoted by ν and N, are expected to be rather large at hadron colliders.

The Hill-Paschos scenario* [5] is based on the assumption that the 4×4 mass matrices m_D and m_M are simultaneously diagonalizable and $m_M = M_0 \mathbf{1}$ lies at the electroweak scale, i.e. $0.1 - 1$ TeV. Then, instead of considering a 6×6 mass matrix, one is left with a 2×2 matrix of the form

$$M_i^\nu = \begin{pmatrix} 0 & m_{D_i} \\ m_{D_i} & M_0 \end{pmatrix} , \tag{25}$$

where the index i runs over all generations. It is obvious that this scenario corresponds effectively to an one-generation model, where the other generations are replicas. Of course,

*This scenario also predicts Majoron fields, whose couplings to fermions may violate astrophysical constraints [23]. However, if $m_{M_{ij}}$ are bare mass terms in the Lagrangian or the gauge group of the SM is extended by an extra hypercharge group, $U(1)_{Y'}$, Majorons will be completely absent in the theory.

the heavy neutrino masses referring to the fourth generation, which are given by

$$m_\nu\,(m_N) \;=\; \frac{1}{2}\,(\sqrt{M_0^2+4m_{D_4}}\;-(+)\;M_0)\;, \tag{26}$$

should have a mass larger than $M_Z/2$ in order to be consistent with the LEP data on neutrino-counting experiments. This can easily be achieved if the naturalness condition $m_{D_i} = \varepsilon_i m_{l_i}$ is assumed (motivated also by certain GUT scenarios [3]), where m_{l_i} is the mass of the ith charged lepton and the constant ε_i is $\mathcal{O}(1)$. For the first three generations $m_{D_i} \ll M_0$ and the light neutrinos do not violate the experimental upper bounds [1]. Nevertheless, the situation becomes different for the fourth generation. The fourth charged lepton E should be rather heavy for phenomenological reasons and may have a mass m_E ($\simeq m_{D_4}$) comparable to M_0. Then, both the neutrinos belonging to this generation, i.e. ν and N, can be quite heavy so as to naturally escape detection at LEP experiments.

Since the lepton mixings can effectively be recovered from the case $n_G = 1$, one has simply to make the following replacements in the differential cross-sections given by Eqs. (8)–(15):

$$B_{l\alpha} \;\to\; B_{l\nu} \text{ or } B_{lN} \qquad \text{and} \qquad C_{\alpha\beta} \;\to\; C_{\nu\nu} \text{ or } C_{NN}. \tag{27}$$

Furthermore, the mixings $C_{\nu\nu}$ and C_{NN} are related with the physical heavy neutrino masses as follows:

$$C_{\nu\nu} \;=\; \frac{m_N}{m_\nu + m_N}\;, \qquad C_{NN} \;=\; \frac{m_\nu}{m_\nu + m_N}. \tag{28}$$

Finally, contributions of 4th generation quarks to the loop functions F^Z and F^H in Eq. (15) should also be considered. Moreover, the possibility of a rather significant modification of Γ_H due to additional decay channels that can open should be taken into account in the production process (H).

III.2 The *LSD* signal and the background analysis

The LSD cross sections in this model crucially depends on the relative magnitudes of m_E, m_ν and m_N. Accordingly one can consider three different possibilities but the dominant contribution to the LSD signal arises from the single or pair production of the ν's and especially if $m_\nu < m_E$.

After making the replacements as pointed out earlier in Section III.1, one finds for the cross section of producing positively and negatively charged LSD's from the process (B) that

$$R_{4G}^{(1)} = \frac{(|B_{e\nu}|^2 + |B_{\mu\nu}|^2)^2}{|B_{e\nu}|^2 + |B_{\mu\nu}|^2 + |B_{\tau\nu}|^2} \leq (s_L^{\nu_e})^2 + (s_L^{\nu_\mu})^2 \,. \tag{29}$$

Thus, we can readily conclude that an analysis similar to Sections II.2 and II.3 should apply to this case and therefore we do not intend to repeat here, too. This also tells us that LSD signals coming from the W-mediated process cannot definitely address the question about the number of neutrino generations.

We next consider the LSD signal from ν-pair production. The dominant process will be the reaction (H). As already discussed in [6], the reason is that the quark-annihilation scattering is $\hat{s}$-channel suppressed relative to (H). On the other hand, the presence of heavy quarks in the triangle graph g$-$g$-H$ enhances coherently the Higgs-exchange cross-section by a factor of 9 if all three heavy quarks are degenerate. Since the fourth-generation up-type quark T and the corresponding down-type one B should almost have equal masses because of constraints resulting from the ρ-parameter or from electroweak oblique parameters [24], the contribution of this additional weak isodoublet to the loop function F^Z will generally be small.

The relevant parameter $R^{(2)}$ defined in Eq. (20) turns out to be

$$R_{4G}^{(2)} = |C_{\nu\nu}|^2 \frac{(|B_{e\nu}|^2 + |B_{\mu\nu}|^2)^2}{(|B_{e\nu}|^2 + |B_{\mu\nu}|^2 + |B_{\tau\nu}|^2)^2} \leq \frac{m_N^2}{(m_\nu + m_N)^2}. \tag{30}$$

In fact, there is no strong upper bound on the parameter $R_{4G}^{(2)}$, which can approach the unity for $m_N \gg m_\nu$ [25]. This is a quite remarkable observation if one compares with numerical results presented in Table I for three-generation models which are suppressed by an additional lepton-violating-mixing factor $(0.02)^2 = 4.\ 10^{-4}$.

As an illustration we have considered the following values for the parameters: $M_0 =$ 100 GeV, $m_E = 320$ GeV and $\varepsilon = 0.75$. This yields $m_\nu = 195$ GeV and $m_N = 295$ GeV. We then compute the LSD cross section (including like-sign e and μ's of both charges in the final state) subject to the kinematical cuts on the leptons discussed in Section III.3 which suffice to remove the background from $t\bar{t}$ production. We have also taken $m_T \simeq m_B = 400$ GeV. The additional decay modes of the Higgs boson leading to a modification of Γ_H, as discussed above, have also been taken into account. The results for LHC (SSC) energies for various Higgs masses (M_H) are displayed in Table IIa (IIb).

Table IIa

M_H [GeV]	No. of events/year
200	$8600 \times R_{4G}^{(2)}$
400	$13300 \times R_{4G}^{(2)}$
600	$34000 \times R_{4G}^{(2)}$
800	$17300 \times R_{4G}^{(2)}$
1000	$7200 \times R_{4G}^{(2)}$

(31)

Table IIb

M_H [GeV]	No. of events/year
200	$1150 \times R_{4G}^{(2)}$
400	$2000 \times R_{4G}^{(2)}$
600	$4200 \times R_{4G}^{(2)}$
800	$2600 \times R_{4G}^{(2)}$
1000	$1050 \times R_{4G}^{(2)}$

(32)

Thus, even with $R_{4G}^{(2)} \simeq 10^{-3}$ a reasonable number of background-free events may be expected at LHC. At SSC, on the other hand, a value of $R_{4G}^{(2)} \simeq 10^{-2}$ may yield an observable LSD signal. The enhancement due to the on-shell production of the Higgs boson and its subsequent decay into ν pairs, as discussed in Ref. [6], can be traced back from the above tables.

In principle, the background arising due to LSD pairs from $T\bar{T}$, $B\bar{B}$ production followed by cascade decays similar to Eq. (22) should also be considered. In the absence of any information about the partial decay rates of T and B a complete analysis cannot be made. However, the following arguments will convince the reader that a substantial background from this channel is not likely to occur:

i) The production cross section of $T\bar{T}$ and $B\bar{B}$ are much suppressed compared to $t\bar{t}$ production. For example, with $m_t = 150$ GeV, $m_T \simeq m_B \simeq 400$ GeV, we have estimated that $\sigma_{T\bar{T}}/\sigma_{t\bar{t}} \simeq 10^{-2}$ at LHC energies.

ii) As a plausible scenario we have assumed that $\mathrm{Br}(T \rightarrow B + X) \simeq 1$ and $\mathrm{Br}(B \rightarrow t + X) \simeq 1$. The LSD signal may then arise through the decay chains

$$T \rightarrow B l^+ \nu_l \qquad \text{and}$$

$$\bar{T} \rightarrow \bar{B} X; \qquad \bar{B} \rightarrow \bar{t} l^+ \nu_l$$

Since the mass difference between T and B cannot be very large for reasons mentioned above, simple decay kinematics will indicate that both the leptons are soft and are not likely to survive the stringent p_T cuts which are, in any case, required to eliminate the background from $t\bar{t}$ pairs. Our Monte-Carlo calculations using $m_T = 400$ GeV, $m_B = 360$ GeV and $m_t = 150$ GeV and kinematical cuts as discussed in section II supports this conclusion.

IV. Conclusions

In this paper we have studied both three and four generation models with heavy Majorana neutrinos, based on the gauge group $SU(2)_L \otimes U(1)_Y$. We have computed all possible cross–sections for the production of such neutrinos, either singly or in pairs, using parton level Monte Carlo. Our calculations reveal that in the three generation model the dominant cross–section is given by the processes (B) and (D) of section II where heavy neutrinos are singly produced in association with a lepton. Lepton number violation arising through the decays of these neutrinos can be detected at the LHC by looking for high p_T LSD pairs ($p_T > 80$ GeV) provided certain mixing angles are not too small compared to their existing upper bounds and the mass of these neutrinos are < 400 GeV. A similar analysis reveals that the isolation of a background free sample of dileptons at SSC is not very likely by looking for high p_T leptons only. In order to do this or to probe larger mass ranges at LHC other features of the signal (e.g., the characteristics of the jets) should be properly utilized. Further studies taking effects like jet fragmentations into account are, therefore, called for.

Calculations in the four generation model reveal that the pair production of these neutrinos through the processes (H) given in section II may also turn out to be the most dominant source of LSD's. This cross section is not suppressed by any small mixing angles but rather depends on the ratio of certain mixing angles. No strong bound on this ratio exists at the moment. Sizable background free LSD samples observable at both LHC and SSC are predicted in this scenario.

Acknowledgements. One of us (AD) wishes to thank Prof. K. Kleinknecht for the kind hospitality in the University of Mainz, FRG.

References

[1] Review of Particle Properties, *Phys. Rev.* **D45** (1992) S1.

[2] T. Yanagida, Proceedings of the *Workshop on Unified Theory and Baryon Number of the Universe*, eds. O. Swada and A. Sugamoto (KEK, 1979) p. 95; M. Gell-Mann, P. Ramond, and R. Slansky, *Supergravity*, eds. P. van Nieuwenhuizen and D. Friedman (North-Holland, Amsterdam, 1979) p. 315.

[3] For reviews see, for example, P. Langacker, *Phys. Rep.* **C72** (1981) 185; R.N. Mohapatra, Unification and Supersymmetry, (Springer–Verlag, New York, 1986).

[4] D.A. Dicus and P. Roy, *Phys. Rev.* **D44** (1991) 1593; W. Buchmüller and C. Greub, *Phys. Lett.* **B256** (1991) 465; *Nucl. Phys.* **B363** (1991) 345; J. Maalampi, K. Mursula and R. Vuopionperä, *Nucl. Phys.* **B363** (1992) 23; D. Choudhury, R.M. Godbole and P. Roy, *Phys. Lett.* **B308** (1993) 394.

[5] C.T. Hill and E.A. Paschos, *Phys. Lett.* **B241** (1990) 96;
C.T. Hill, M.A. Luty and E.A. Paschos, *Phys. Rev.* **D43** (1991) 3011; G. Jungman and M.A. Luty, *Nucl. Phys.* **B361** (1991) 24.

[6] A. Datta and A. Pilaftsis, *Phys. Lett.* **B278** (1992) 162.

[7] W. Buchmüller and D. Wyler, *Phys. Lett.* **B249** (1990) 458.

[8] P. Langacker and D. London, *Phys. Rev.* **D38** (1988) 886.

[9] G. Bhattacharyya etal., *Mod. Phys. Lett.* **A6** (1991) 2921; E. Nardi, E. Roulet and D. Tommasini, *Nucl. Phys.* **B386** (1992) 239.

[10] A. Pilaftsis, *Z. Phys.* **C55** (1992) 275.

[11] A. Pilaftsis, *Phys. Lett.* **B285** (1992) 68; J.G. Körner, A. Pilaftsis and K. Schilcher, *Phys. Rev.* **D47** (1993) 1080; *Phys. Lett.* **B300** (1993) 381; J. Bernabéu, J.G. Körner, A. Pilaftsis and K. Schilcher, *Phys. Rev. Lett.* **71** (1993) 2695.

[12] See, for instance, S. Dawson and S. Willenbrock, *Phys. Lett.* **B211** (1988) 200.

[13] A. Martin, R. Roberts and J. Stirling, *Phys. Rev.* **D43** (1991) 3648.

[14] S. Dawson, *Nucl. Phys.* **B249** (1984) 42.

[15] P.W. Johnson, F.J. Olness and W.-K. Tung, *Phys. Rev.* **D36** (1987) 291; R.M. Godbole, S.D. Rindani, *Phys. Lett.* **B190** (1987) 192.

[16] see Fig. 4 of R.P. Kauffman, *Phys. Rev.* **D41** (1990) 3343. Also, Table II of this work shows that the analytical expressions for the relevant for us subprocess reactions will not have any hard relative dependence of $\sqrt{\hat{s}}$ but only a very soft one which is logarithmic. This clearly indicates that the numerical results of Fig. 4 will qualitatively be still valid for energies $\sqrt{\hat{s}} \gg 2$ TeV.

[17] D.A. Dicus, M. Karatas, P. Roy, *Phys. Rev.* **D44** (1991) 2033.

[18] A. Datta, M. Guchait and D.P. Roy, *Phys. Rev.* **D47** (1993) 961.

[19] R.M. Godbole, S. Pakvasa, D.P. Roy, *Phys. Rev. Lett.* **50** (1983) 1539; V. Barger, A. Martin and R.J.N. Phillips, *Phys. Rev.* **D28** (1983) 145.

[20] D.P. Roy, *Phys. Lett.* **B196** (1987) 395.

[21] F.E. Paige and S.D. Protopopesu, *ISAJET* program, Brookhaven preprint BNL-38034 (1986).

[22] N.K. Mondal and D.P. Roy, TIFR preprint, TIFR/TH/93-23.

[23] R.N. Mohapatra and X. Zhang, *Phys. Lett.* **B305** (1993) 106.

[24] M.E. Peskin and T. Takeuchi, *Phys. Rev. Lett.* **65** (1990) 964; *Phys. Rev.* **D46** (1992) 381; G. Altarelli and R. Barbieri, *Phys. Lett.* **B253** (1990) 161; G. Altarelli, R. Barbieri and S. Jadach, *Nucl. Phys.* **B369** (1992) 3.

[25] In fact, the mass parameters m_E, m_ν and m_N cannot be arbitrarily large, since they are restricted by renormalization-group-triviality bounds (see also [5]) and constraints from electroweak oblique parameters. The latter has been discussed by
S. Bertolini and A. Sirlin, *Phys. Lett.* **B257** (1991) 179; E. Gates and J. Terning, *Phys. Rev. Lett.* **67** (1991) 1840; B.A. Kniehl and H.-G. Kohrs, *Phys. Rev.* **D48** (1993) 225.

Figure Captions

Fig. 1: Feynman graphs responsible for the subprocess (A): $W_L W_L \to l^+ l^+$.

Fig. 2: Feynman graphs relevant for the singly heavy Majorana neutrino production, i.e. processes (B), (C) and (D) (see also text).

Fig. 3: Feynman diagrams relevant for double heavy Majorana neutrino production as described by the processes (E)–(H) in Section II.2

Fig. 4: Missing transverse momentum distribution of the SM background (see also Eq. (22)).

Fig. 5: Transverse momentum distribution of the softer lepton p_{T2} coming from the SM background. For comparison, we have considered the p_{T2} distribution of the LSD signal which predominantly originates from the process (B).

Table I. Numerical estimates of production cross sections for the processes (A)-(H) leading to LSD signals in the context of three-generation models.

Process	$m_N = 200 - 1000$ GeV LHC $(\sqrt{s} = 16)$ TeV σ_{tot} [pb]	$m_N = 200 - 1000$ GeV SSC $(\sqrt{s} = 16)$ TeV σ_{tot} [pb]
A.	$< 5.\ 10^{-2} \times R^{(1)2}$	$< 1.\ 10^{-1} \times R^{(1)2}$
B.	$1. - 2.\ 10^{-3} \times R^{(1)}$	$15. - 3.\ 10^{-2} \times R^{(1)}$
C.	small, $\mathcal{O}(R^{(1)3})$	small, $\mathcal{O}(R^{(1)3})$
D.	$3.\ 10^{-3} \times R^{(1)}$	$4.5\ 10^{-2} \times R^{(1)}$
E.	$5.\ (10^{-4} - 10^{-6}) \times R^{(2)}$	$(10^{-3} - 10^{-5}) \times R^{(2)}$
F.	$(2.5\ 10^{-4} - 5.\ 10^{-3}) \times R^{(2)}$	$(3.\ 10^{-3} - 8.\ 10^{-2}) \times R^{(2)}$
G.	$(2.\ 10^{-4} - 4.\ 10^{-3}) \times R^{(2)}$	$(2.5\ 10^{-3} - 7.\ 10^{-2}) \times R^{(2)}$
H.	$5.\ (10^{-3} - 10^{-5}) \times R^{(2)}$	$4.5\ (10^{-2} - 10^{-4}) \times R^{(2)}$

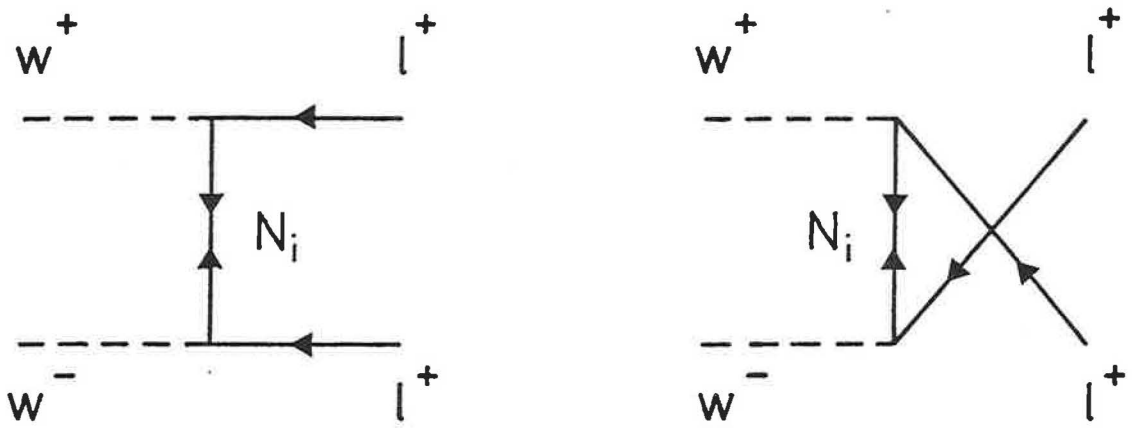

Fig. 1

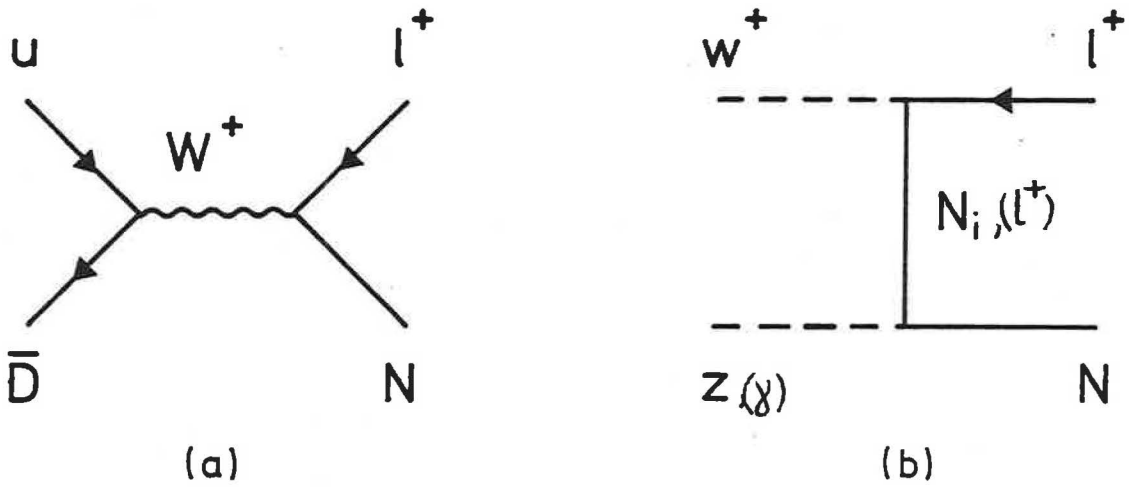

Fig. 2

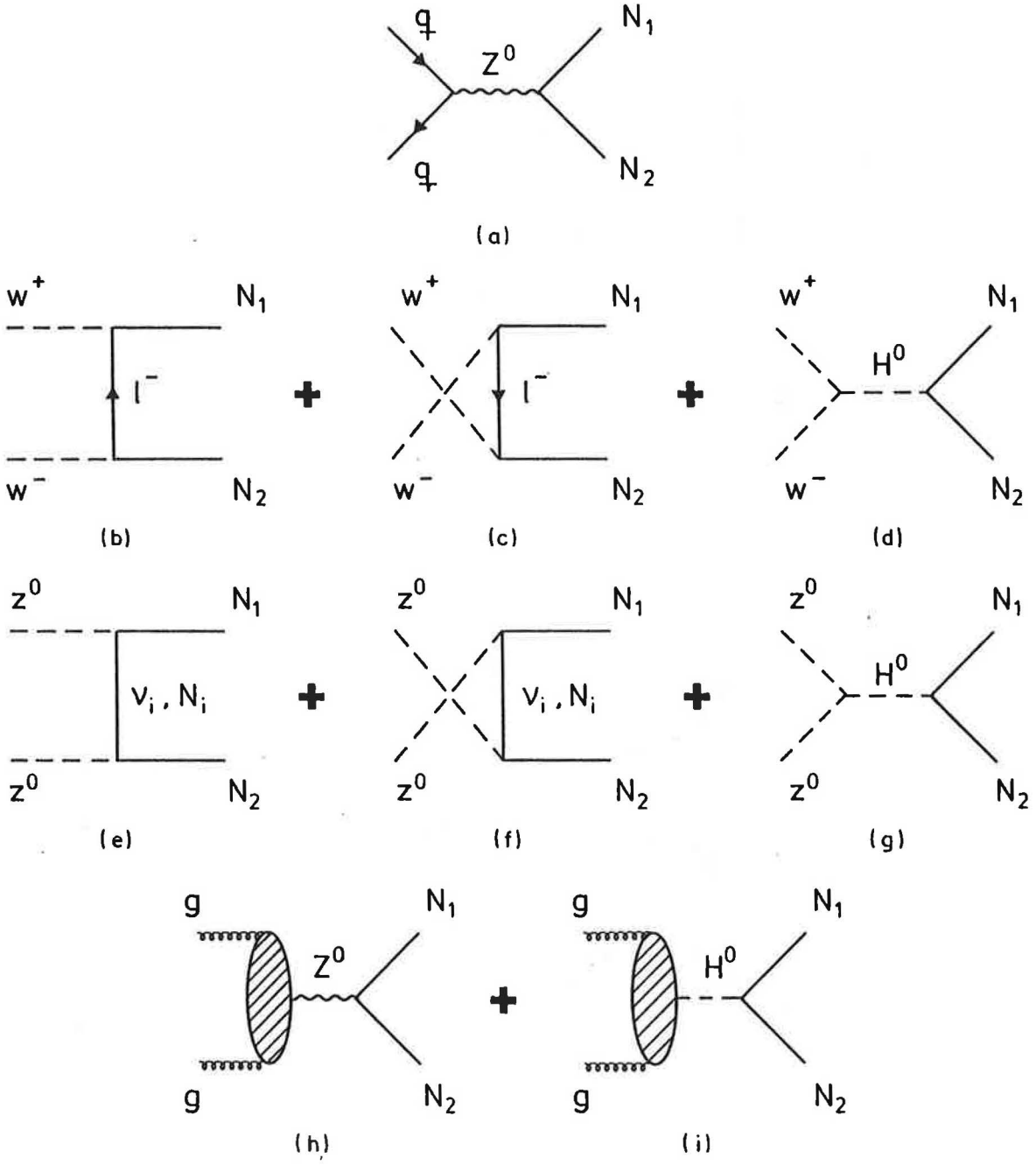

Fig. 3

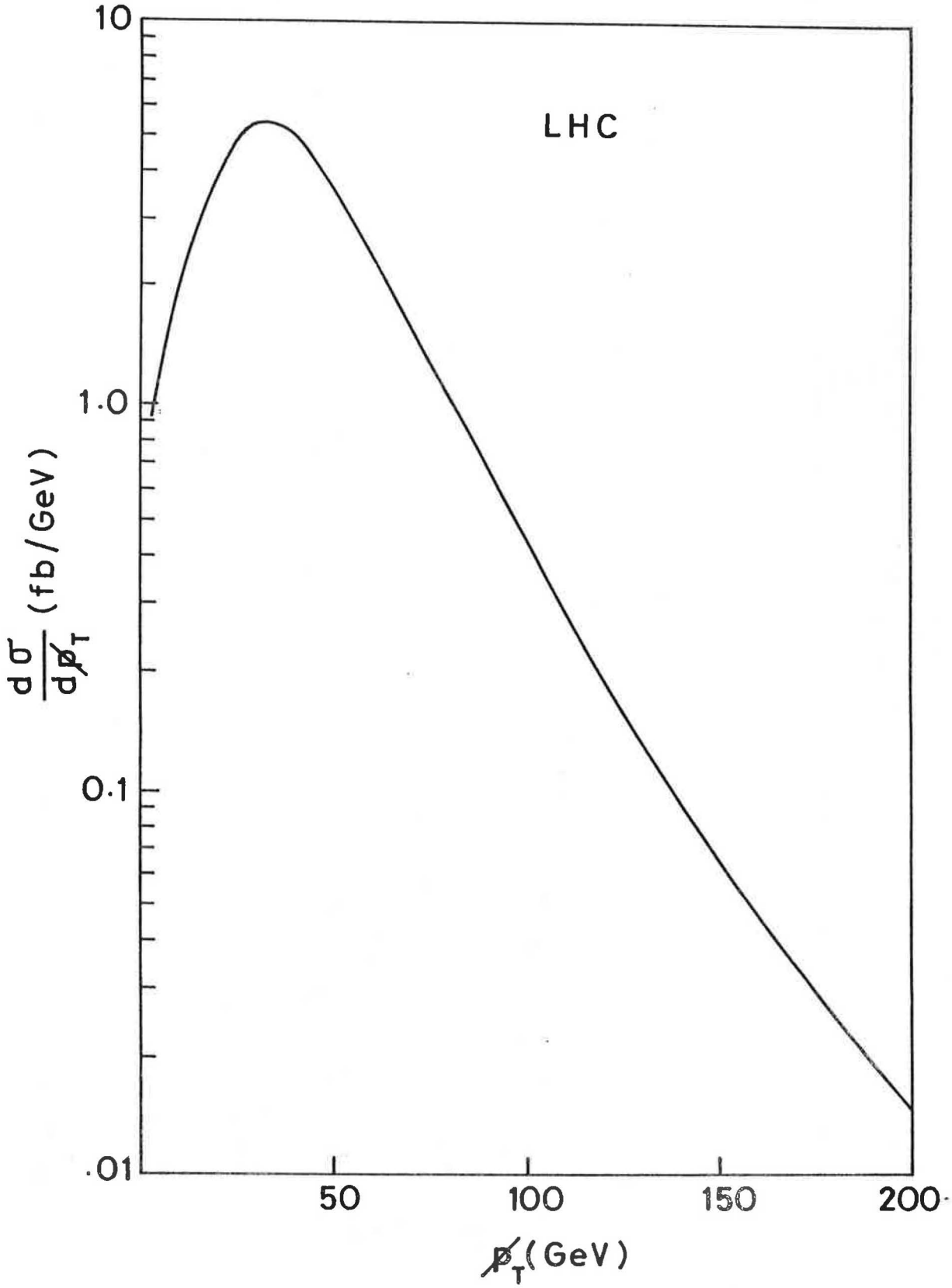
10
1·0
0·1
·01
LHC
$\frac{d\sigma}{d\not{p}_T}$ (fb/GeV)
50
100
150
200
$\not{p}_T$ (GeV)

Fig. 4.

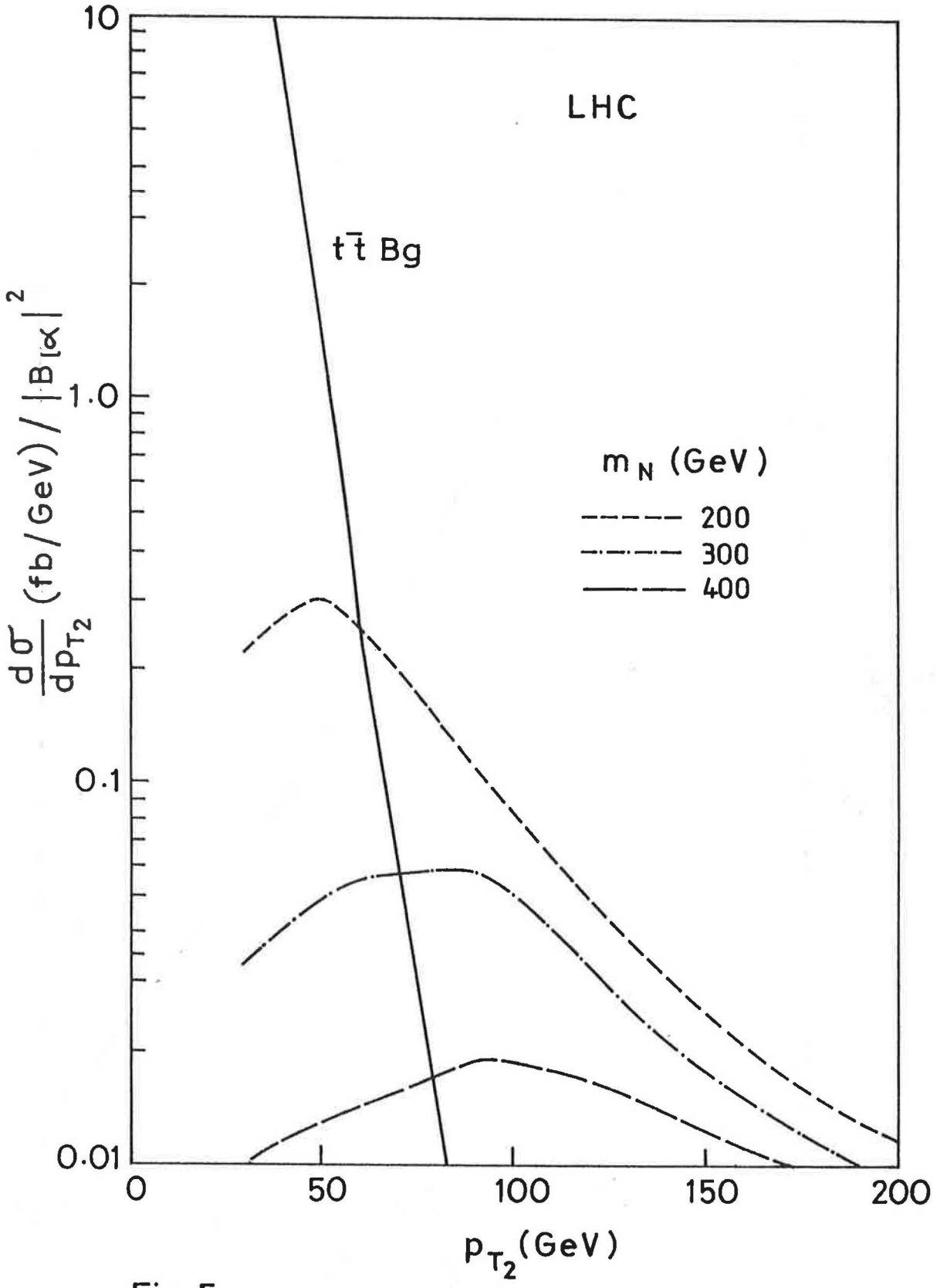
LHC
$t\bar{t}$ Bg
m_N (GeV)
200
300
400
$\frac{d\sigma}{dp_{T_2}}$ (fb/GeV) / $|B(\alpha)|^2$
10
1.0
0.1
0.01
0
50
100
150
200
p_{T_2} (GeV)

Fig. 5.